thermal vibrations have not been considered. For the map including reflections up to 1·20 Å^{-1} (close to the refinement limit) conceptual model errors will be balanced as much as possible by changes in the IA parameters $\mathbf{r}_p$ and $\mathbf{U}_p$. It is therefore not surprising that the 1·20 Å^{-1} map shows only random noise. Balancing is less complete, however, when the reflection set is limited to $(\sin\theta)/\lambda = 1{\cdot}00$ Å^{-1}. Especially for the 1·00 Å^{-1} DIF(**r**) map series-termination peaks due to model errors can thus be expected.

3.2 *Filtered deformation densities*

The deformation features extracted from the data by the multipole refinements are given [*cf.* (2)] by

$$\mathrm{DEF}_{\mathrm{exp}}(\mathbf{r}) \equiv \mathrm{DEF}(\mathrm{model};\mathbf{r}). \qquad (5)$$

As discussed above, $\mathrm{DEF}_{\mathrm{exp}}(\mathbf{r})$ only shows low-resolution deformations. Random errors in $\mathrm{DEF}_{\mathrm{exp}}(\mathbf{r})$ caused by the standard deviations in the deformation parameters are predominantly due to the $\sigma(F_o)$'s of the low-order reflections. For BCP, $\sigma_{\mathrm{ar}}(0{\cdot}65) = 0{\cdot}007$ e Å^{-3} is taken as a reasonable estimate for $\sigma_{\mathrm{ar}}[\mathrm{DEF}_{\mathrm{exp}}(\mathbf{r})]$, for regions $> 0{\cdot}4$ Å from the nuclei. Close to the nuclei the standard deviations will be higher owing to the influence of random errors in the IA parameters on DEF(model;**r**). For VCP with correlations (Table 4) and IA standard deviations comparable to BCP, the BCP $\sigma_{\mathrm{ar}}[\mathrm{DEF}_{\mathrm{exp}}(\mathbf{r})]$ value has also been accepted. For CP this σ_{ar} value is multiplied by a factor of two because of the larger correlation coefficients and IA standard deviations. Standard deviations at positions containing (pseudo-)symmetry elements are found by multiplying σ_{ar} by $\sqrt{2}$ for each available (pseudo-) symmetry element.

The $\mathrm{DEF}_{\mathrm{exp}}(\mathbf{r})$ maps of Fig. 5 and C—C bond peak heights listed in Table 2 are obtained by Fourier summation of the reflections up to $(\sin\theta)/\lambda = 1{\cdot}00$ Å^{-1}. The sections of the ring plane (Figs. 5*a,b,c*) clearly reveal the bent bond character of the ring C—C bonds. The sections perpendicular to and through the centre of the central bonds in BCP and VCP, and of the double bond in VCP show the expected deviation from a circular density distribution, which increases going from the 'single' bond in BCP *via* the 'single' bond in VCP to the double bond in VCP. A further discussion of the deformation densities will be given on the basis of the static deformation densities in paper III.

The computations were carried out at the Computing Centre of the University of Groningen. The investigations were supported in part by the Netherlands Foundation for Chemical Research (SON) with financial aid from the Netherlands Organization for the Advancement of Pure Research (ZWO).

References

BASTIANSEN, O., FRITSCH, F. N. & HEDBERG, K. (1964). *Acta Cryst.* **17**, 538–543.

BECKER, P. J. & COPPENS, P. (1974). *Acta Cryst.* A**30**, 129–147.

BENTLEY, J. & STEWART, R. F. (1976). *Acta Cryst.* A**32**, 910–914.

CLEMENTI, E. (1965). *Tables of Atomic Functions.* San José Research Laboratory, International Business Machines Corporation, San José, California, USA.

COX, E. G. & CRUICKSHANK, D. W. J. (1948). *Acta Cryst.* **1**, 92–93.

HAGEN, K., HAGEN, G. & TRÆTTEBERG, M. (1972). *Acta Chem. Scand.* **26**, 3649–3661.

HAMILTON, W. C. (1965). *Acta Cryst.* **18**, 502–510.

HEHRE, W. J., STEWART R. F. & POPLE, J. A. (1969). *J. Chem. Phys.* **51**, 2657–2664.

KEULEN, E. (1969). PhD Thesis. Univ. of Groningen, The Netherlands.

LEVIN, I. W. & PEARCE, R. A. R. (1978). *J. Chem. Phys.* **69**, 2196–2208.

NES, G. J. H. VAN & VAN BOLHUIS, F. (1979). *Acta Cryst.* B**35**, 2580–2593.

NIJVELDT, D. & VOS, A. (1988*a*). *Acta Cryst.* B**44**, 281–289.

NIJVELDT, D. & VOS, A. (1988*b*). *Acta Cryst.* B**44**, 296–307.

STEWART, R. F., BENTLEY, J. & GOODMAN, B. (1975). *J. Chem. Phys.* **63**, 3786–3793.

STEWART, R. F. & SPACKMAN, M. A. (1981). *VALRAY Users Manual.* Preliminary draft. Department of Chemistry, Carnegie–Mellon Univ., Pittsburgh, PA, USA.

TRÆTTEBERG, M. (1983). Private communication.

WAL, R. VAN DER (1982). PhD Thesis. Univ. of Groningen, The Netherlands.

Acta Cryst. (1988). B**44**, 296–307

Single-Crystal X-ray Geometries and Electron Density Distributions of Cyclopropane, Bicyclopropyl and Vinylcyclopropane. III. Evidence for Conjugation in Vinylcyclopropane and Bicyclopropyl

BY DICK NIJVELDT AND AAFJE VOS

Laboratory of Chemical Physics, University of Groningen, Nijenborgh 16, 9747 *AG Groningen, The Netherlands*

(*Received* 21 *November* 1986; *accepted* 9 *December* 1987)

Abstract

Starting from the qualitative Walsh model for cyclopropane (CP), a discussion is given on the influence of (possible) conjugation on the geometry and electron density distribution of bicyclopropyl (BCP) and vinylcyclopropane (VCP). Conjugation is expected to induce, for example, (i) geometric ring asymmetry and

0108-7681/88/030296-12$03.00

(ii) extension of the electron density at the central C–C bonds in the π direction (to be denoted by the asymmetry parameter ap). In the density study, X-ray deformation model densities, based upon diffuse deformation functions and $\mathbf{U} = 0$, are compared with static deformation densities obtained by *ab initio* quantum theoretical SCF–LCAO–MO calculations. Use of extended (EG) basis sets including polarization functions turned out to be necessary. Possible inadequacies of the theoretical EG densities could not be detected with certainty by the density analysis of the present volatile compounds. Theoretical EG densities yield equal ap values for the central C–C bonds in BCP and VCP. For VCP, the presence of conjugation is supported by the observed asymmetry of the ring, in which the distal bond is 0·0145 (7) Å shorter than the adjacent bonds. For BCP, ring asymmetry has not been found. Although ring asymmetry for BCP is expected to be smaller than for VCP and can (partly) be disguised by libration effects on the observed bond lengths, its absence is hard to explain if conjugation in BCP and VCP is equally strong.

1. Introduction

The possible existence of conjugation in vinylcyclopropane (VCP) and in bicyclopropyl (BCP) will be discussed on the basis of the X-ray geometries and deformation densities determined in the first two papers of the present series (Nijveldt & Vos, 1988*a*,*b*; hereinafter referred to as papers I and II respectively). The qualitative Walsh (1949) molecular orbital model to be discussed in the next section, will be applied for the discussion of the geometrical data. Experimental deformation densities with **U** set to zero will be compared with static densities obtained by quantum chemical calculations. In these calculations the nuclei are fixed at their experimental positions.

2. Qualitative theoretical model for conjugation

2.1. *Unsaturated character of cyclopropane*

Essential for conjugation in VCP and BCP is the unsaturated character of the cyclopropyl group. The unsaturated character of cyclopropane (CP) is indicated by its analogy with unsaturated compounds like ethene C_2H_4 and ethyne C_2H_2. This similarity is, for instance, shown by (i) addition of HBr and Br_2 to CP (Von Baeyer, 1885), (ii) the bond lengths and angles observed by electron diffraction [ED; $\langle C-H\rangle = 1{\cdot}089\ (3)$ Å, $\langle H-C-H\rangle = 115{\cdot}1\ (10)°$; Bastiansen, Fritsch & Hedberg (1964)] and (iii) the existence of weak hydrogen-bonded complexes CP···H–X (halogen) with H–X in the plane of the ring perpendicular to C–C and pointing to the midpoint of C–C [X = F, Buxton, Aldrich, Shea, Legon & Flygare (1981); X = Cl, Legon, Aldrich & Flygare (1982)].

2.2. *The Walsh model for cyclopropane*

A qualitative molecular orbital (MO) description for CP is given by the Walsh (1949) model which is based on the analogy between CP and ethene. Each CP C atom contains one sp^2 and one p orbital in the plane of the ring, in addition to two sp^2 hybridized atomic orbitals (AO's) localized along the C–H bonds. The ring-plane AO's combine to give the following MO's (Fig. 1).

$$4e_A = 2^{-1/2}(sp_2^2 - sp_3^2) \quad (1a)$$

$$4e_S = 6^{-1/2}(2sp_1^2 - sp_2^2 - sp_3^2) \quad (1b)$$

$$3a_1 = 3^{-1/2}(sp_1^2 + sp_2^2 + sp_3^2) \quad (1c)$$

$$1a_2 = 3^{-1/2}(p_1 + p_2 + p_3) \quad (2a)$$

$$3e_A = 6^{-1/2}(2p_1 - p_2 - p_3) \quad (2b)$$

$$3e_S = 2^{-1/2}(p_2 - p_3). \quad (2c)$$

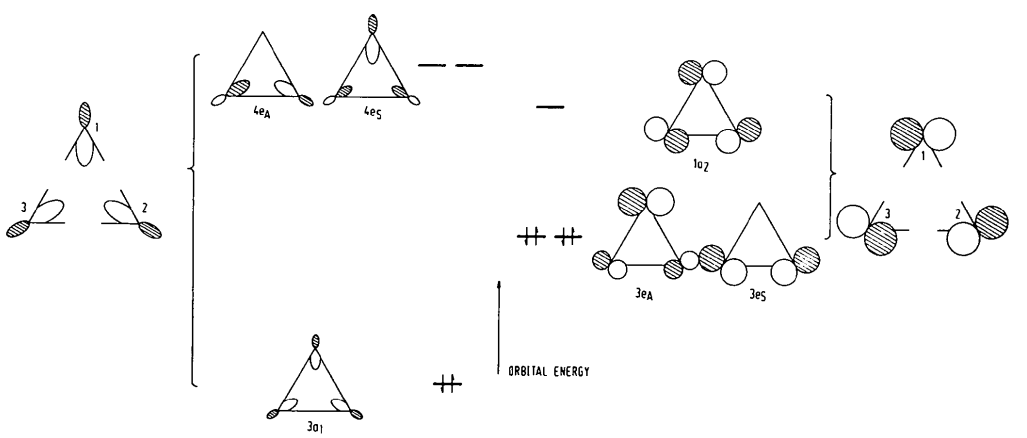

Fig. 1. Walsh orbitals in the plane of the CP ring (see text).

The AO subscripts 1–3 refer to the three C atoms; the indices *A* or *S* of the degenerate MO's symbolize antisymmetry or symmetry with respect to the mirror plane perpendicular to the ring and bisecting the endocyclic angle at atom 1. The sequence of the MO energy levels in Fig. 1 is in agreement with the assignment of UV absorption bands by Meyer & Pasternak (1977). In an earlier paper by Basch, Robin, Kuebler, Baker & Turner (1969) the $3e$ and $4e$ orbitals were supposed to be the highest occupied (HO) and lowest vacant (LV) MO's, respectively.

2.3. *Conjugation in vinylcyclopropane*

In the Walsh picture, the central C(1)–C(4) bond in VCP (Fig. 2*a*) is formed by a σ-type combination of the two sp^2 hybridized AO's of C(1) and C(4) along C(1)–C(4). In the *trans*-bisected conformation, observed in the crystal and preferred in the gas phase, the $3e_A$ HOMO and the $1a_2$ and $4e_A$ LVMO of CP have correct symmetry to interact with the π HOMO and π^* LVMO of ethene. Interaction between the HOMO's is considerable. Orbital splitting measured by photoelectron spectroscopy [PES; Bruckmann & Klessinger (1974)] gives, in Hückel MO (HMO) approximation, $\beta = -2{\cdot}12$ eV for the resonance integral between the C(1) and C(4) p orbitals. The relative orbital energies in the qualitative picture of Fig. 2(*b*) are taken from the above PES study ($-10{\cdot}6$ for $3e_A$ and $-10{\cdot}25$ eV for π, taken equal in the picture) and from UV absorption spectra [CP: $3e \rightarrow 1a_2$ 7·8 eV, Meyer & Pasternak (1977); ethene: $\pi \rightarrow \pi^*$ 7·7 eV, Murai (1952)]. Orbital $4e_A$ has tentatively been drawn at the same level as $1a_2$, since Basch *et al.* (1969) have assigned the CP 7·8 eV transition to $3e \rightarrow 4e$. The coefficients of the MO's in (1) and (2) show that overlap between $3e_A$ and π^* is larger than between $1a_2$ and π, indicating that the $3e_A$–π^* interaction gives the major contribution to conjugation in VCP.

In view of the Walsh MO model (Fig. 1) and the above considerations, conjugation is expected to have the following consequences for VCP.

1. Preference for the (*cis*- or *trans*-) bisected conformation.

2. A net electron flow from the cyclopropyl group to the central and double bond.

3. Shortening of the distal [C(2)–C(3), paper I Fig. 3*c*] and lengthening of the adjacent [C(1)–C(2) and C(1)–C(3), paper I Fig. 3*c*] bond(s) due to the withdrawal of electron density from the CP $3e_A$ orbital, which has antibonding character for the distal and bonding character for the adjacent bond(s).

4. Increase/decrease in bonding character for the central/double bond.

5. Elongation of the deformation density at the central bond in the π direction (perpendicular to symmetry plane of *trans*- or *cis*-bisected conformation).

Physical evidence for conjugation in VCP and in related compounds is available in the literature.

(i) Microwave spectroscopy yields a dipole moment of $1{\cdot}66 \times 10^{-30}$ C m (Codding & Schwendeman, 1974), in reasonable agreement with a theoretical value of $1{\cdot}43 \times 10^{-30}$ C m [electron density flow from ring; Skancke & Boggs (1979)].

(ii) Preference for the *trans*-bisected form in the gas phase and in solution is shown by different types of experiment [^{1}H NMR: De Maré & Lapaille (1980); ED: Trætteberg (1983); Raman: Carreira, Towns & Malloy (1978)] and by *ab initio* calculations. Inclusion of geometry optimization for each rotation angle around the central bond and use of sufficiently large split-valence basis sets is necessary (Skancke & Boggs, 1979; De Maré & Peterson, 1982; Huang & Pan, 1984).

(iii) X-ray diffraction reveals ring asymmetry. At the start of the present study measurements of ring asymmetry were available only for VCP-related compounds with –C=C=O attached to the CP ring. Observed values for the ring asymmetry δ, defined by

$$\delta = \langle(\text{C–C; ring})\rangle - (\text{C–C; distal}), \qquad (3)$$

are: $\delta = +0{\cdot}027\,(4)$ Å (Overbeek, Olthof, van der Putten & Schenk, 1978) and $\delta = +0{\cdot}020\,(5)$ Å (Maslen, Toia, White & Willis, 1975). Quantum

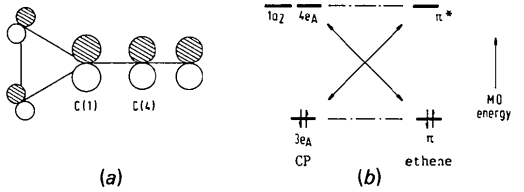

Fig. 2. *trans*-Bisected conformation of VCP. (*a*) Walsh MO picture of the bonding combination of the HOMO's $3e_A$ and π. (*b*) Schematic correlation diagram between the HOMO's and the relevant LVMO's of CP and ethene. For the choice of the different levels, see text.

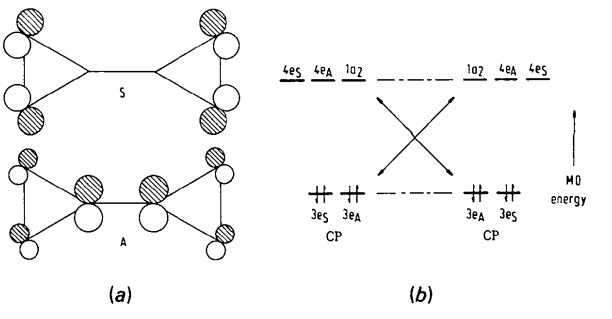

Fig. 3. *trans*-Bisected conformation of BCP. (*a*) Walsh picture of the antisymmetric (*A*) and symmetric (*S*) bonding combinations of the HOMO's $3e_A$ and $3e_S$ respectively. (*b*) Schematic correlation diagram between all CP HOMO's and LVMO's. The energy levels are in agreement with the levels of Fig. 2.

theoretical calculations on VCP itself gave $\delta = +0.007$ Å (De Maré & Peterson, 1982) and $\delta = +0.012$ Å (Huang & Pan, 1984).

2.4. *Conjugation in bicyclopropyl*

The bonding combinations of the two Walsh HOMO's of CP are depicted for the *trans*-bisected BCP conformation in Fig. 3(*a*). According to PES (Von Asmus & Klessinger, 1976), interaction between HOMO's of type $3e_S$ (splitting 0·9 eV) is considerably smaller than for type $3e_A$ (splitting 2·3 eV). In HMO approximation the resonance integral $\beta = -1.74$ eV for the considered p orbitals of the central bond atoms. The coefficients of the MO's of (1) and (2) show that the $3e_A$–$1a_2$ combination is the most favourable one for BCP in the (*trans*- or *cis*-) bisected form. Conjugation in BCP is expected to be notably smaller than in VCP because of the increase in $|\beta|$ in the order BCP < VCP < butadiene[$|\beta| = 2.43$ eV; Bruckmann & Klessinger (1974)].

Consequences of the described conjugation for BCP are:

1. Preference for the bisected conformation.
2. Increase of the density on the central bond.
3. Decrease of electron density in $3e_A$ and increase in $1a_2$. This results in a lengthening of the adjacent bonds for both orbital types, while the distal bonds are lengthened in $1a_2$ and (slightly) shortened in $3e_A$.
4. Extension of the density at the central bond in the direction perpendicular to the symmetry plane of the (*trans*-) bisected conformation.

Convincing physical evidence for the presence of conjugation in BCP is not available in the literature. In contrast with VCP, for BCP in the gas phase and in solution the *gauche* form is slightly more favourable than the *trans*-bisected form [ED: Hagen, Hagen & Trætteberg (1972); IR: de Meijere, Lüttke & Heinrich (1974); PES plus MINDO: Von Asmus & Klessinger (1976)]. This supports the expectation that possible conjugation in BCP is smaller than in VCP.

3. Geometry

3.1. *Available bond lengths and angles*

The ultimate multipole (UM) model described in paper II, § 2.7, is considered to be the most reliable model for each of the compounds. Positional and thermal parameters are given in Table 1; bond lengths and angles are listed in Table 2.* Note that C–H directions are taken from UM-type refinements with 'normal' H replaced by polarized H, while C–H bond lengths are derived from ED values (paper II, § 2.4).

Table 1. *Fractional atomic coordinates* (× 10^5; *for* H × 10^4) *and equivalent isotropic thermal parameters* U_{eq} (10^{-5} Å^2; *for* H 10^{-3} Å^2)

UM coordinates corrected for rigid-body libration are given under UM*. The e.s.d.'s of the H-atom positional parameters are retrieved from the corresponding multipole refinements with positionally free polarized H atoms (*cf.* paper II, § 2.4).

$$U_{eq} = \tfrac{1}{3}\sum_i\sum_j U_{ij} a_i^* a_j^* \mathbf{a}_i.\mathbf{a}_j.$$

	Type	Atom	x	y	z	U_{eq}
CP	UM	C(1)	0	30567 (10)	0	2533 (13)
	UM	C(2)	9407 (5)	17928 (7)	17057 (16)	2593 (8)
	UM	H(3)	0	4650 (15)	279 (30)	44 (7)
	UM	H(4)	0	2547 (23)	1741 (23)	42 (7)
	UM	H(5)	1577 (10)	471 (11)	1099 (16)	47 (6)
	UM	H(6)	1586 (10)	2540 (14)	3083 (15)	48 (5)
BCP	UM	C(1)	0	−331 (4)	6360 (2)	1655 (4)
	UM	C(2)	8498 (2)	20387 (4)	12892 (2)	2134 (4)
	UM	H(3)	0	−1971 (14)	1005 (7)	34 (3)
	UM	H(4)	1428 (7)	3566 (11)	802 (6)	41 (3)
	UM	H(5)	1389 (7)	1442 (12)	2071 (4)	40 (2)
VCP	UM	C(1)	8062 (4)	−1490	−21369 (3)	1612 (3)
	UM*	C(1)	8079	−1522	−21390	
	UM	C(2)	−2479 (6)	11576 (5)	−38951 (4)	2151 (5)
	UM*	C(2)	−2465	11627	−39022	
	UM	C(3)	−23141 (5)	−603 (5)	−32126 (4)	2120 (5)
	UM*	C(3)	−23272	−632	−32149	
	UM	C(4)	17767 (5)	6517 (5)	−1142 (3)	1839 (4)
	UM*	C(4)	17777	6541	−1098	
	UM	C(5)	39456 (6)	1 (6)	13225 (4)	2477 (5)
	UM*	C(5)	39546	−14	13295	
	UM	H(6)	1951 (14)	−1386 (9)	−2424 (12)	25 (2)
	UM*	H(6)	1960	−1397	−2429	
	UM	H(7)	258 (18)	805 (14)	−5279 (10)	34 (3)
	UM*	H(7)	267	807	−5292	
	UM	H(8)	−220 (20)	2662 (10)	−3560 (14)	37 (3)
	UM*	H(8)	−219	2677	−3566	
	UM	H(9)	−3194 (20)	−1247 (11)	−4145 (12)	37 (3)
	UM*	H(9)	−3210	−1258	−4150	
	UM	H(10)	−3703 (16)	574 (15)	−2432 (12)	38 (3)
	UM*	H(10)	−3730	575	−2430	
	UM	H(11)	622 (13)	1883 (9)	189 (11)	35 (3)
	UM*	H(11)	616	1893	196	
	UM	H(12)	5187 (15)	−1178 (10)	1091 (13)	42 (3)
	UM*	H(12)	5204	−1187	1096	
	UM	H(13)	4518 (16)	684 (11)	2746 (9)	39 (3)
	UM*	H(13)	4526	687	2758	

For CP and BCP, a rigid-body analysis of the C-atom **U** tensors with the translation, libration and screw (**TLS**) tensor program (Schomaker & Trueblood, 1968) resulted in unrealistic negative values for at least one component of the libration tensor. For VCP, which has the smallest (pseudo-) symmetry, results of the **TLS** analysis are presented in Fig. 4. Considerable internal rotation around the VCP central bond has been excluded on the basis of (i) the noncoincidence of L_1 and the central bond (angle 32°), and (ii) the $\mathbf{U}_o$–$\mathbf{U}_c$ values after the **TLS** analysis.

VCP parameters corrected for libration are given with an asterisk (Tables 1 and 2). Also asterisked are ED bond lengths which have been reduced by 0·001 Å as it is known that ED bond lengths tend to be *ca* 0·001 Å longer than X-ray bond lengths corrected for libration [examples: VCP, compare ⟨C–C; UM*⟩

* Lists of anisotropic thermal parameters for the three molecules have been deposited with the British Library Document Supply Centre as Supplementary Publication No. SUP 44635 (2 pp.). Copies may be obtained through The Executive Secretary, International Union of Crystallography, 5 Abbey Square, Chester CH1 2HU, England.

Table 2. *Bond lengths* (Å) *and angles* (°) *which are not included in Fig.* 5

All values refer to the UM model, except for VCP–UM* where the UM values corrected for rigid-body libration are listed. The e.s.d.'s are in accordance with the deviations given in Table 1.

CP		BCP	
C(1)–C(2)	1·4988 (8)	C(1)–C(1′)	1·4924 (4)
C(2)–C(2′)	1·4997 (11)	C(1)–C(2)	1·5052 (3)
C(1)–H(3)	1·060 (10)	C(2)–C(2′)	1·5046 (4)
C(1)–H(4)	1·071 (13)	C(1)–H(3)	1·077 (7)
C(2)–H(5)	1·067 (8)	C(2)–H(4)	1·092 (6)
C(2)–H(6)	1·074 (9)	C(2)–H(5)	1·078 (5)
C(2)–C(1)–H(3)	116·5 (8)	C(1′)–C(1)–C(2)	119·54 (2)
C(2)–C(1)–H(4)	117·3 (7)	C(2)–C(1)–H(3)	115·9 (3)
C(1)–C(2)–H(5)	117·9 (5)	C(1)–C(2)–H(4)	117·8 (3)
C(1)–C(2)–H(6)	119·0 (5)	C(1)–C(2)–H(5)	117·2 (3)
C(2′)–C(2)–H(5)	118·4 (4)	C(2′)–C(2)–H(4)	117·9 (3)
C(2′)–C(2)–H(6)	118·6 (4)	C(2′)–C(2)–H(5)	116·3 (3)

VCP					
	UM	UM*		UM	UM*
C(1)–C(2)	1·5153 (4)	1·5215	C(2)–C(1)–C(4)	118·78 (2)	118·59
C(1)–C(3)	1·5123 (4)	1·5187	C(3)–C(1)–C(4)	119·05 (2)	118·85
C(1)–C(4)	1·4728 (4)	1·4783	C(2)–C(1)–H(6)	115·9 (4)	116·0
C(2)–C(3)	1·4993 (5)	1·5096	C(3)–C(1)–H(6)	116·2 (3)	116·2
C(4)–C(5)	1·3340 (4)	1·3383	H(7)–C(2)–H(8)	115·0 (8)	115·0
C(1)–H(6)	1·093 (7)	1·100	C(1)–C(2)–H(7)	117·4 (5)	117·3
C(2)–H(7)	1·080 (8)	1·086	C(1)–C(2)–H(8)	116·9 (5)	117·0
C(2)–H(8)	1·102 (7)	1·109	C(3)–C(2)–H(7)	118·1 (5)	118·2
C(3)–H(9)	1·086 (8)	1·092	C(3)–C(2)–H(8)	118·4 (6)	118·4
C(3)–H(10)	1·071 (10)	1·079	H(9)–C(3)–H(10)	115·3 (7)	115·3
C(4)–H(11)	1·096 (7)	1·103	C(1)–C(3)–H(9)	116·9 (5)	116·7
C(5)–H(12)	1·075 (8)	1·082	C(1)–C(3)–H(10)	117·2 (4)	117·4
C(5)–H(13)	1·071 (7)	1·075	C(2)–C(3)–H(9)	117·5 (5)	117·6
			C(2)–C(3)–H(10)	118·5 (6)	118·6

from Table 2 with ⟨C–C; ED⟩ = 1·474 Å from Trætteberg (1983); dibenzene chromium, Keulen (1969)]. The σ's of the X-ray values given in parentheses refer to random errors only and thus give no indication of the uncertainties in the corrections applied to obtain the asterisked values.

The average librational shortening of the VCP C–C ring bond lengths is 0·0076 Å. The thermal motions of the ring C atoms with mean values $\langle U_{eq}(\mathrm{VCP})\rangle = 0{\cdot}0196$, $\langle U_{eq}(\mathrm{BCP})\rangle = 0{\cdot}0197$ and $\langle U_{eq}(\mathrm{CP})\rangle = 0{\cdot}0257$ Å^2, give rise to the expectation that, on average, the librational shortening of the ring-bond lengths increases in the order BCP ≈ VCP < CP.

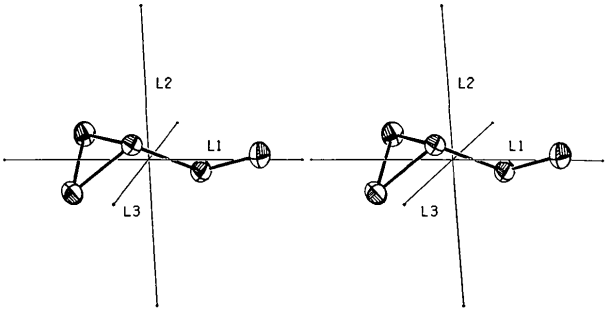

Fig. 4. Stereographic drawing of the ultimate multipole VCP C skeleton in the libration coordinate system. Thermal ellipsoids are given at 50% probability level (Johnson, 1976). Magnitudes of libration are $\omega_{11} = 0{\cdot}0110$, $\omega_{22} = 0{\cdot}0030$ and $\omega_{33} = 0{\cdot}0021$ rad^2.

3.2. *Geometry description*

CH_2 *groups of the ring.* In each of the three compounds the plane of the ring clearly exhibits mirror symmetry for all C(ring)H_2 groups (see Fig. 5 and Table 2). In CP and BCP the HCH planes bisect the adjacent endocyclic C–C–C angle. In VCP, the HCH planes are rotated out of their bisecting positions, away from the distal bond, by 1·8 (9) and 1·7 (8)° around the normal to the ring plane. This possibly significant rotation with an average value of 1·8 (6)° will be discussed in §3.3.

Average C–C *ring-bond lengths.* In VCP the average length of the C–C ring bonds is 0·0040 (4) Å larger than in BCP, whereas in CP this average length is 0·0059 (8) Å smaller than in BCP. It cannot be excluded that the latter decrease is due (mainly) to the relatively large librational shortening expected for CP. The lengthening of 0·0040 (4) Å in VCP with respect to BCP is considered to be physically real, since the average librational shortening of the ring bonds in BCP and VCP is expected to be the same.

Ring asymmetry. The VCP ring shows distal shortening. The ring asymmetry δ defined by (3) reduces from $\delta = 0{\cdot}0097$ (3) to $\delta = 0{\cdot}0070$ (3)* Å when libration correction is applied. The observed asymmetry in BCP, $\delta = 0{\cdot}0004$ (2) Å, is not significant.

Geometry around the central bonds. In terms of the Walsh model described in §2.2, the hybridization state of a ring C atom is determined by the angles ψ between the exocyclic bonds and the plane of the ring. The angles at the C atoms of the central bonds in BCP and VCP shown in Fig. 5 indicate that the same hybridization character can be assumed for the C atoms of the two central bonds. The small decrease of ψ (central bond) by 0·89 (6)° and the reduction in central-bond length by 0·0196 (6) Å in VCP with respect to BCP will be discussed in the next section.

3.3. *Evidence for conjugation*

VCP shows several geometrical features which are characteristic for conjugation.

1. Ring-bond asymmetry, $\delta = 0{\cdot}0070$ (3)* Å. The shortening of the distal bond is supported by the average rotation of 1·8 (6)° of the two ring HCH groups, away from the distal bond. If the HCH planes were not rotated, the nonbonded distances H(*p*)···C(2 or 3) would have been 0·011* Å shorter on average than the distances H(*p*)···C(1). The observed differences between H(*p*)···C(2 or 3) and H(*p*)···C(1) range from 0·001* to 0·005* Å.

2. Elongation by 0·0086 (4) Å of the adjacent ring bonds in VCP with respect to BCP points to a larger conjugation in the former molecule.

3. Reduction by 0·89 (6)° of ψ(central bond) with respect to BCP. According to § 2.3 conjugation in VCP causes a net electron density flow from the ring to the vinyl group, which diminishes the repulsion between the ring and the central-bond density.

The central-bond lengths in BCP, VCP and butadiene show a regular decrease; with use of the same libration correction for BCP as for VCP, the respective values are 1·4979 (4)*, 1·4783 (4)* and 1·462 (3)* Å [ED: Kuchitsu, Fukuyama & Morino (1968)]. With the assumption that the hybridization of the central-bond C atoms is the same in the three compounds, the drop is an inseparable combination of decreasing nonbonded repulsion and increasing conjugation.

A small, although not significant, increase is observed for the lengths of the double bonds in the series ethene [1·3374 (10)* Å observed by ED: Duncan (1974)], VCP [1·3383 (4)* Å] and butadiene [1·340 (2)* Å]. The small increase does not contradict the assumption of increasing conjugation in the series, since bond orders of double bonds are influenced less by conjugation than bond orders of single bonds [*cf.* butadiene in Coulson (1972)].

In contrast with VCP, the available geometrical data do not give conclusive evidence for the presence of conjugation in BCP since

(*a*) Ring asymmetry, which is expected to be smaller than in VCP, has not been observed.

(*b*) Average ring-bond lengthening with respect to CP cannot be detected because of librational uncertainties.

(*c*) It cannot be decided (yet) whether the central bond is shortened due to conjugation, because, apart from VCP, accurate lengths are not available for bonds which might serve as reference states. Even if such information were known, it would be difficult to separate influences of changing conjugation, nonbonded repulsion and hybridization on the bond lengths.

In view of the above discussion, for BCP the decision on the presence of conjugation requires, within the scope of the present work, a study of the complete electron density distribution.

4. Theoretical deformation densities

4.1. *Computations*

Quantum theoretical *ab initio* calculations have been performed for the individual molecules, with neglect of environmental influence in the respective crystals. The calculations of the molecular densities ρ_{th}(molecule,**r**) with the program *BIGMOL* (Thole & van Duijnen, 1979) are based upon the SCF–LCAO–MO method of Roothaan (1951). The nuclei are fixed at UM positions $\mathbf{r}_p$, which in the case of VCP were corrected for libration.

First a 'small Gaussian' (SG) double-ζ basis set of contracted Gaussian functions (4*s*, 2*p*/2*s*) was taken,

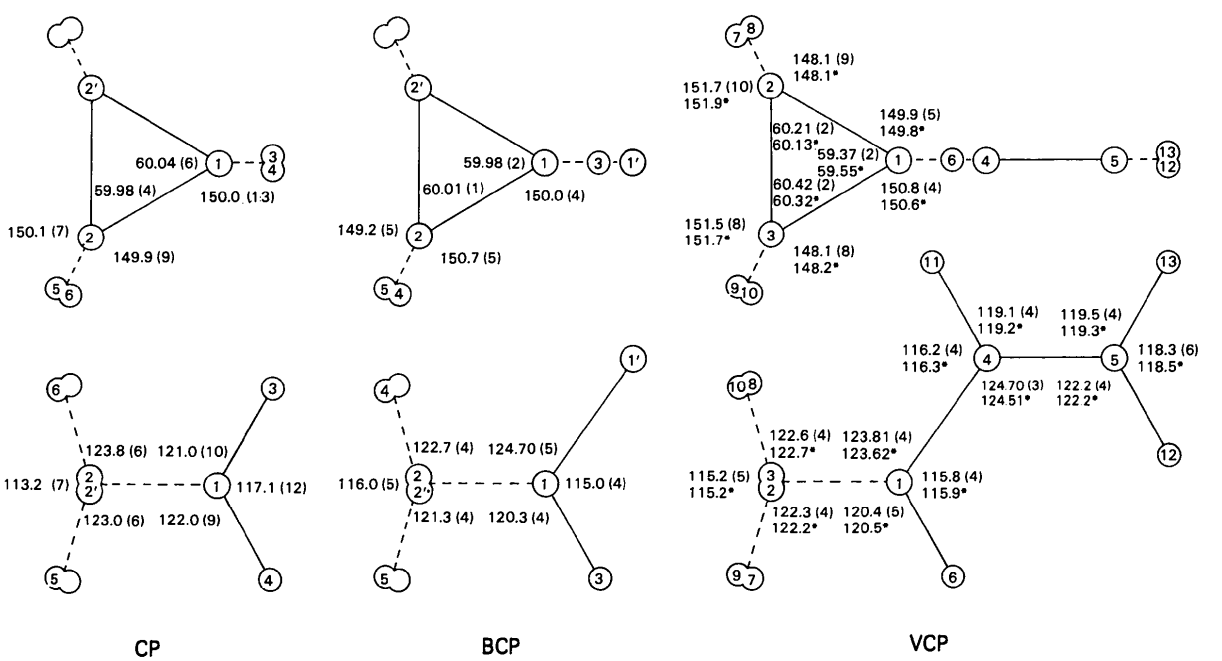

Fig. 5. Angles between bonds or between bonds and adjacent planes (°). Asterisked values have been corrected for rigid-body libration. Above: Projection along the normal to the ring plane. Exocyclic angles are between C–C ring bond and HCH or HCC plane. Below: Projection down the distal bond. Values above and below the ring plane refer to the angles between the exocyclic bond and the ring plane. Values at the left side of the ring refer to the H–C–H angles. At the distal bond of VCP average values of the angles related by the pseudo-mirror plane are given.

including for C the Roos & Siegbahn (1970*a*) (7*s*, 3*p*) atomic basis set and for H the (3*s*) set of van der Velde (1974). After that, the basis set was extended with polarization functions according to Roos & Siegbahn (1970*b*), yielding the (4*s*, 2*p*, 1*d*/2*s*, 1*p*), or shortly the EG, basis set.

The theoretical static deformation density is given by

$$\mathrm{DEF}^{o}_{\mathrm{th}}(\mathbf{r}) = \rho_{\mathrm{th}}(\mathrm{molecule};\mathbf{r}) - \sum_p \rho^{p}_{\mathrm{th}}(\mathrm{IA},\mathbf{r}_p;R_p). \quad (4)$$

The (spherically averaged) independent-atom (IA) densities are retrieved directly from the given atomic basis sets, since the coefficients of these sets are derived from optimizations on the respective free atoms.

4.2. *Results*

In Fig. 6, density sections of CP for the SG and EG basis sets are compared. Heights of SG and EG maxima on C–C and density values at the ring centres are listed in Table 3 for the three compounds. The most striking changes caused by the addition of polarization functions are: (i) introduction of detailed deformation features, (ii) increase in height of bond deformation peaks, (iii) increase of the deformation density at the ring centres to a positive value, and (iv) increase of the density gradients at the H nuclei.

Figs. 7(*a*), (*b*), (*c*) illustrate that the EG deformation densities of the ring planes in the three compounds show only minor differences. According to Table 4, EG deformation peaks at the C–H bonds vary only little. Some sections containing C–H bonds are given in Figs. 7(*d*), (*e*), (*f*).

5. Experimental deformation densities

5.1. *Character of* $DEF^{o}_{exp}(\mathbf{r})$ *maps*

The experimental dynamic $\mathrm{DEF}_{\mathrm{exp}}(\mathbf{r})$ maps (defined in paper II, §3) have been subjected to the transformations

$$\mathrm{DEF}_{\mathrm{exp}}(\mathbf{r}) \rightarrow \mathrm{DEF}^{o}_{\mathrm{exp}}(\mathbf{r}) \rightarrow \mathrm{DEF}^{o}_{\mathrm{exp,H}}(\mathbf{r}). \quad (5)$$

In the first step the maps are made static by setting $\mathbf{U} = 0$. The second step replaces the contracted H atom used in the experimental IA reference model by the free H atom applied in the theoretical reference model.

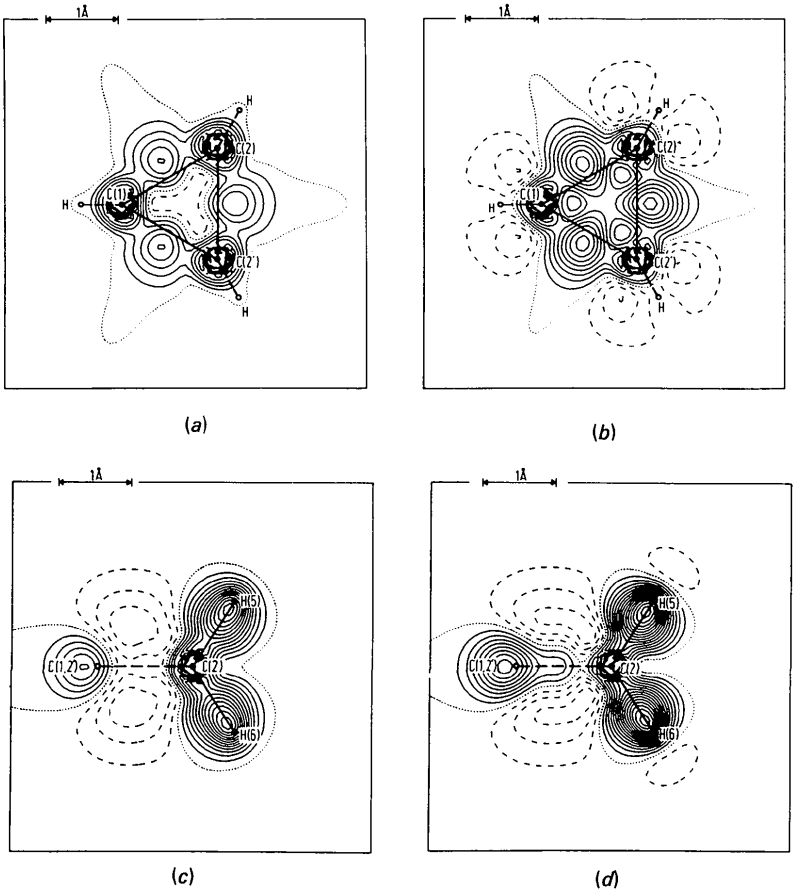

Fig. 6. $\mathrm{DEF}^{o}_{\mathrm{th}}(\mathbf{r})$ maps for sections through the ring and the C(2)H(5)H(6) plane of CP. (*a*), (*c*) SG basis set. (*b*), (*d*) EG basis set. Contours here and in the following DEF^{o} maps are at intervals of 0·05 e Å^{-3}; full lines give positive, dotted lines zero and dashed lines negative contours.

Table 3. *Static deformation densities*

The two theoretical models are indicated by SG for the small and by EG for the extended basis set. The experimental model is indicated by UM. The column headings are: DEF^o_{max} the maximum of the density (4) or (5) at a bond or in the centre of the ring; bba the bent bond angle, defined as the angle between the line connecting two ring C atoms and the line through the density maximum of the corresponding bond and one of the two atoms; ap the asymmetry parameter which is the ratio between the density half-value widths along the π direction and perpendicular to the π direction at the midpoint of a C–C bond (§6.3). The units are: DEF^o_{max} (10^{-2} e Å^{-3}) and bba (°).

		C–C; adjacent		C–C; distal		Ring centre	C–C; central		C–C; double	
	Type	DEF^o_{max}	bba	DEF^o_{max}	bba	DEF^o_{max}	DEF^o_{max}	ap	DEF^o_{max}	ap
CP	SG	25	17			−7				
	EG	43	14			13				
	UM	36 (4)	15 (1) C(2)–C(2′)			14 (4)				
		37 (3)	13 (1) C(1)–C(2)							
BCP	SG	28	17	26	17	−7	39	1·06		
	EG	44	14	43	14	13	58	1·06		
	UM	38 (1)	13 (1)	33 (1·5)	16 (1)	9 (1·5)	47 (2)	1·09 (4)		
VCP	SG	26	17	25	17	−6	40	1·06	62	1·35
	EG	42	14	43	14	13	61	1·06	77	1·49
	UM	37 (1)	16 (1) C(1)–C(2)	35 (1·5)	16 (1)	11 (1·5)	56 (1·5)	1·18 (2)	75 (1·5)	1·32 (2)
		36 (1)	16 (1) C(1)–C(3)							

The $DEF^o_{exp,H}(\mathbf{r})$ maps only show the diffuse features of the deformation density. As discussed in paper II, §1, deformation functions revealing sharp high-resolution features could not be applied because of the limited $(\sin\theta)/\lambda$ range of the data and the thermal smearing. For the calculation of the $DEF^o_{exp,H}(\mathbf{r})$ maps reflections up to $(\sin\theta)/\lambda = 1{\cdot}4$ Å^{-1} are included.

Carbon correlation coefficients $|\rho_C|$ between static deformation parameters and remaining parameters are <0·50 for BCP and VCP (paper II, Table 4), indicating

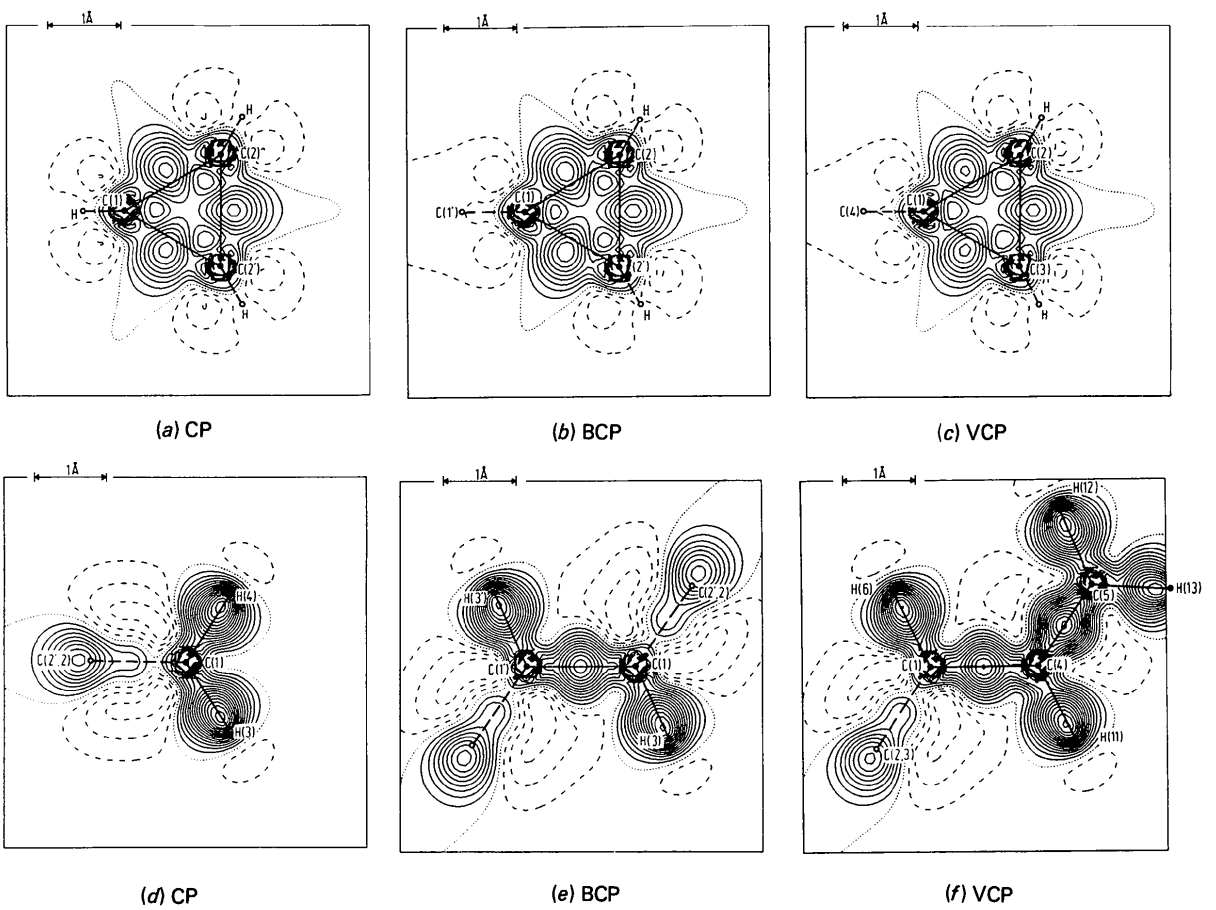

Fig. 7. Sections of $DEF^o_{th}(\mathbf{r})$ maps from the EG basis set. (*a*), (*b*), (*c*) Ring planes; the minimum density of the dips at a distance of 0·4 Å from the C nuclei at the line bisecting the endocyclic angle is *ca* 0·02 e Å^{-3}. (*d*) CP: C(1)H(4)H(3) plane. (*e*) BCP: C(1)C(1′)H(3′) plane. (*f*) VCP: C(1)C(4)C(5) plane.

that the diffuse static deformation features have been filtered reliably from the data. For CP with some $|\rho_C| > 0{\cdot}50$, filtering is less perfect.

The standard deviations in $DEF^o_{exp,H}(\mathbf{r})$ are obtained by multiplying $\sigma[DEF_{exp}(\mathbf{r})]$ (*cf.* paper II, §3) by $\exp[8\pi^2 U_{eq}\langle(\sin\theta)/\lambda\rangle^2]$, with $U_{eq} = 0{\cdot}02$ Å^2 and $\langle(\sin\theta)/\lambda\rangle = 0{\cdot}49$ Å^{-1}. In this way, approximate account is taken of the increase in random errors due to the sharpening of the deformation densities. The resulting standard deviations σ^o_{ar} at arbitrary positions more than 0·4 Å remote from any of the nuclei are 0·01 e Å^{-3} for BCP and VCP and 0·02 e Å^{-3} for CP. At a (pseudo-) special position a multiplication factor of $\sqrt{2}$ is required for each (pseudo-) symmetry element.

The influence of errors in the (constrained) l(C–H) values on the dipole deformations at H has been determined by performing refinements for BCP with l(C–H) increased or decreased by 0·02 Å. Absolute values of changes in bond maxima on C–H or minima beyond C–H are <0·048 e Å^{-3}. Possible errors in the librational shortening, which was assumed to be 0·02 Å for the constrained C–H values (paper II, §2.4), will thus hardly influence the deformation density maps.

Table 4. *$DEF^o(\mathbf{r})$ extreme peak values for the different* C–H *bonds in the three compounds*

Minimum and maximum values, in units of 0·05 e Å^{-3}, are given for the positive peaks at C–H ($^+$) and for the negative peaks beyond H ($^-$).

	$DEF^o_{th}(\mathbf{r})$				$DEF^o_{exp,H}(\mathbf{r})$			
Compound	min$^+$	max$^+$	min$^-$	max$^-$	min$^+$	max$^+$	min$^-$	max$^-$
CP	+15	+15	−1	−1	+14	+15	−3	−2
BCP	+14	+15	−1	−1	+14	+14	−2	−2
VCP	+14	+15	−1	−1	+12	+14	−3	−2

5.2. *Comparison of ring planes and* C–H *bonds*

In view of the e.s.d.'s and the uncertainties in regions <0·4 Å remote from the nuclei, $DEF^o_{exp,H}(\mathbf{r})$ sections through the ring planes of the three compounds do not show differences to which physical significance can be attached (Figs. 8*a,b,c*; Table 3). The same holds for the

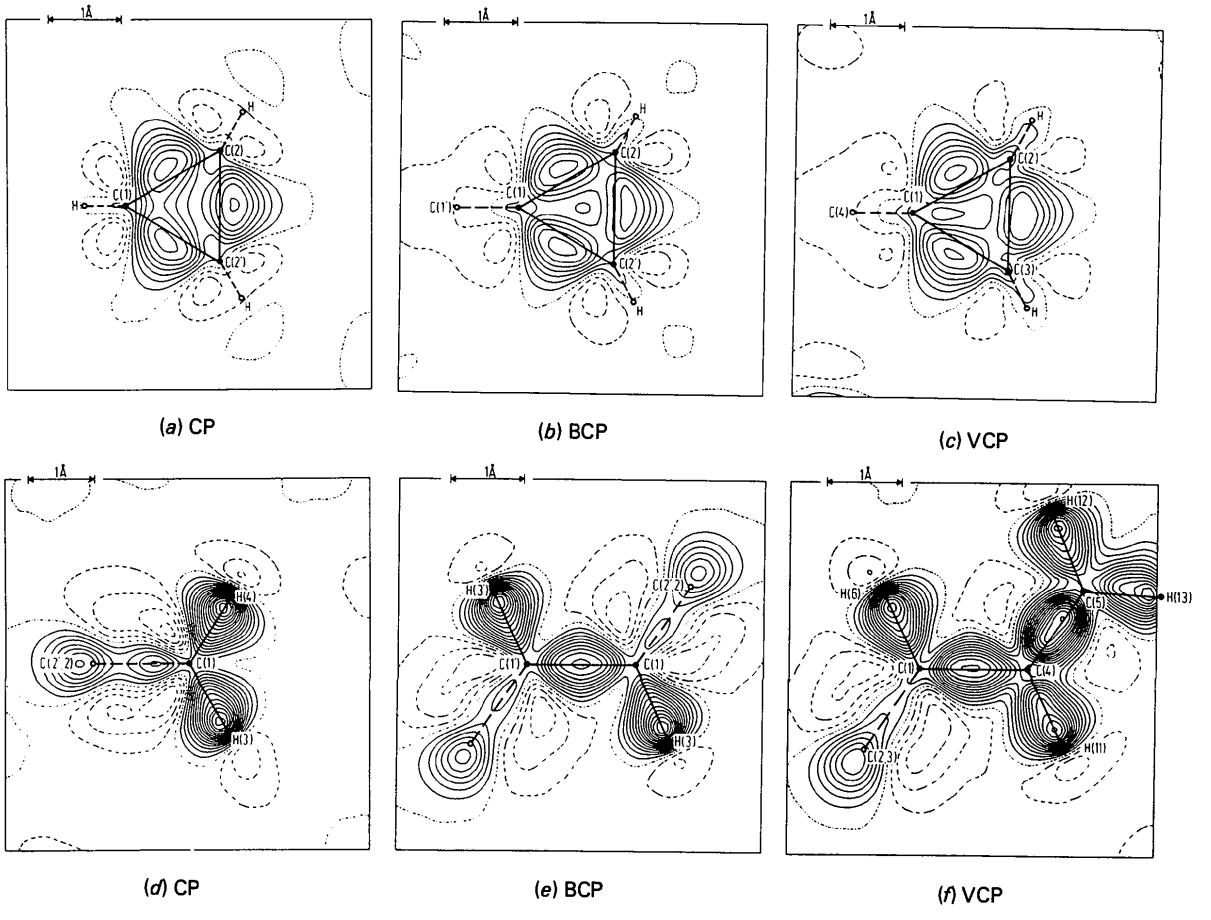

Fig. 8. Sections of $DEF^o_{exp,H}(\mathbf{r})$ maps. (*a*), (*b*), (*c*) Ring planes. (*d*) CP: C(1)H(4)H(3) plane. (*e*) BCP: C(1)C(1′)H(3′) plane. (*f*) VCP: C(1)C(4)C(5) plane.

deformations on the C—H bonds (Figs. 8*d,e,f*; Table 4). For VCP which reveals the largest variation in C—H bond maxima, the difference of 0·07 e Å^{-3} between the extreme values is 3·5 times the σ(difference) estimated on the basis of random F_o errors only.

6. Discussion

6.1. *The essential contribution of polarization functions*

Comparison of the experimental and theoretical SG and EG maps (Figs. 8 and 6; Table 3) reveals that the EG maps approach the experimental maps much better than do the SG maps. For the present compounds, this emphasizes the necessity of including polarization functions in theoretical *ab initio* calculations.

6.2. *Restrictions of the* $DEF^o_{exp,H}(\mathbf{r})$ *maps*

In Fig. 9, experimental and theoretical EG deformation density line sections through the BCP plane are compared. The sections clearly show the diffuse character of the $DEF^o_{exp,H}(\mathbf{r})$ maps. Although the experimental density gives a good smoothed representation of the theoretical density, details like the dips at 0·4 Å from the C nuclei [shown at the C(1) projection in Fig. 9(*b*) and at 0·4 Å from C(2) in Fig. 9(*c*)] are missing in the experimental maps. Because of their diffuse character, the $DEF^o_{exp,H}(\mathbf{r})$ maps for the ring planes fail to show whether the EG theoretical density still shows shortcomings. For the C—H bonds the agreement between experiment and theory is as good as for the ring planes, in spite of the assumptions made for H (paper II, § 2.4).

6.3. *Central- and double-bond asymmetries*

The possible deviations from cylindrical symmetry of the densities at the exocyclic C—C bonds (§2.3 and 2.4) are a source of information on conjugation. Sections perpendicular to and through the midpoints of these bonds are shown in Fig. 10 for $DEF^o_{exp,H}(\mathbf{r})$ and $DEF^o_{th,EG}(\mathbf{r})$. As expected, extension of the density in the π direction is clearly present for the VCP double bond. For the central bonds this extension is notably less. Numerical information is given by the asymmetry parameters ap defined and listed in Table 3.

Introduction of polarization functions (*d* orbitals for C) during the theoretical calculations does not change the central-bond ap values, but enhances the double-bond ap of VCP. This increase can be ascribed to a relatively strong occupation and/or extension of *d* orbitals in the region of the double-bond π electrons. The SG ap parameters of the central bonds in BCP and VCP are the same. This contradicts the qualitative discussion of § 2, which predicts a larger conjugation for VCP than for BCP.

The experimental BCP central-bond ap is equal to the theoretical parameter. In case of VCP the central-bond ap is larger, whereas the double-bond ap is smaller than the corresponding theoretical value of the EG model. The relatively large experimental VCP central-bond ap does not necessarily imply that the qualitative theoretical discussion of § 2 is essentially correct and

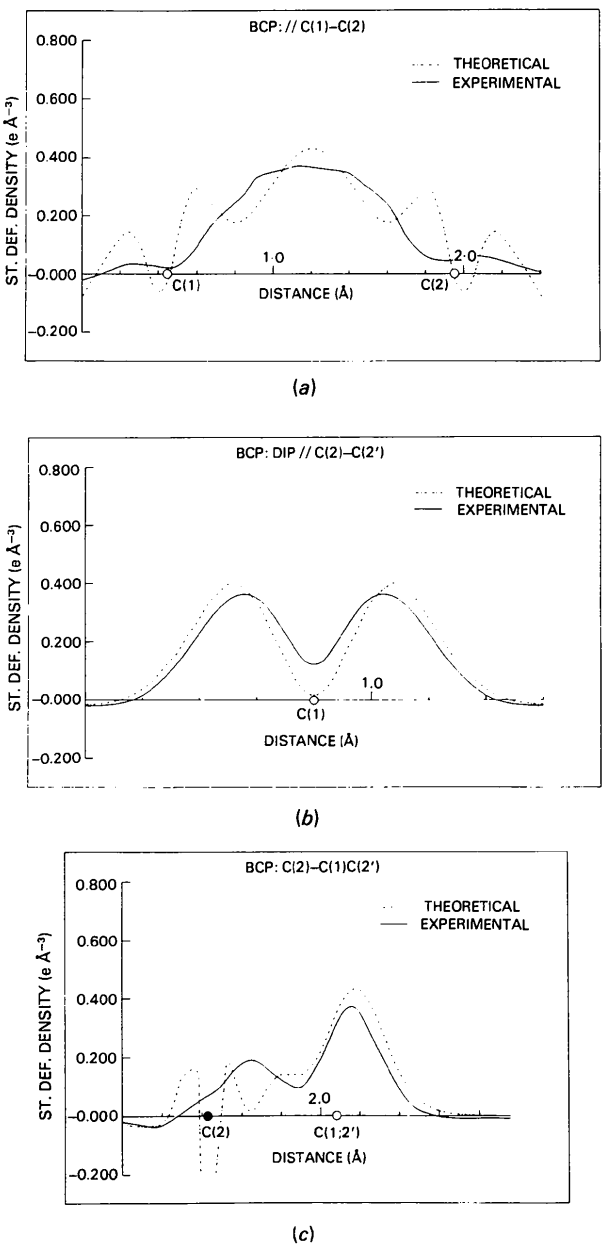

Fig. 9. BCP $DEF^o_{th,EG}(\mathbf{r})$ and $DEF^o_{exp,H}(\mathbf{r})$ profiles. (*a*) Parellel to C(1)—C(2) and through the density maximum of this bond. (*b*) Through the theoretical dip near C(1) and parallel to the opposite bond. (*c*) Through C(2) and the centre of the opposite bond. C atoms are indicated by • and projections of C's by ○.

that the EG ap parameters are not reliable. Shortcomings of the semi-empirical qualitative model are, for example, (i) its rigidity owing to the use of localized C(sp^2) orbitals for the exocyclic bonds, and (ii) the failure to explain the splitting of 0·9 e V observed by PES for the BCP $3e_S$ orbital. Moreover, it cannot be excluded that the experimental VCP ap's contain systematic errors owing to restrictions for multipole refinement parameters, necessitated by the limited information content of the data set (finite measuring accuracy, limited resolution). Firstly, application of simple Slater-type functions (paper II, §2.1) for the radial distributions and use of the same exponent for multipoles of the same type hampers detection of a possible relatively strong extension of *d* orbitals in the double-bond π-electron region. Secondly, double- and central-bond ap's may be correlated *via* the finite series of multipoles centred at C(4). Note that (i) the sum ap(central) + ap(double) in VCP is the same within experimental error for experiment and EG theory, and (ii) the *noncentrosymmetry* of the VCP crystals makes it hard to detect refinement-model inadequacies from ρ_o(crystal;**r**) − ρ(model;**r**) residual density maps because of the use of model phases for ρ_o(crystal;**r**).

6.4. *Concluding remarks*

Possible shortcomings of the EG theoretical densities could not be detected with certainty by the density analysis of the present volatile compounds. In terms of the qualitative model described in §2, the EG model renders an almost equally strong conjugation in BCP and VCP. For VCP, conjugation is revealed clearly by the geometric ring asymmetry (§3.3). In contrast with this, geometric ring asymmetry has not been observed for BCP. Although ring asymmetry for BCP is expected to be smaller than for VCP and can partly be masked by the influence of libration on the observed bond lengths, its absence is hard to explain if conjugation in BCP is as strong as in VCP.

The computations were carried out at the Computing Centre of the University of Groningen. The investigations were supported in part by the Netherlands

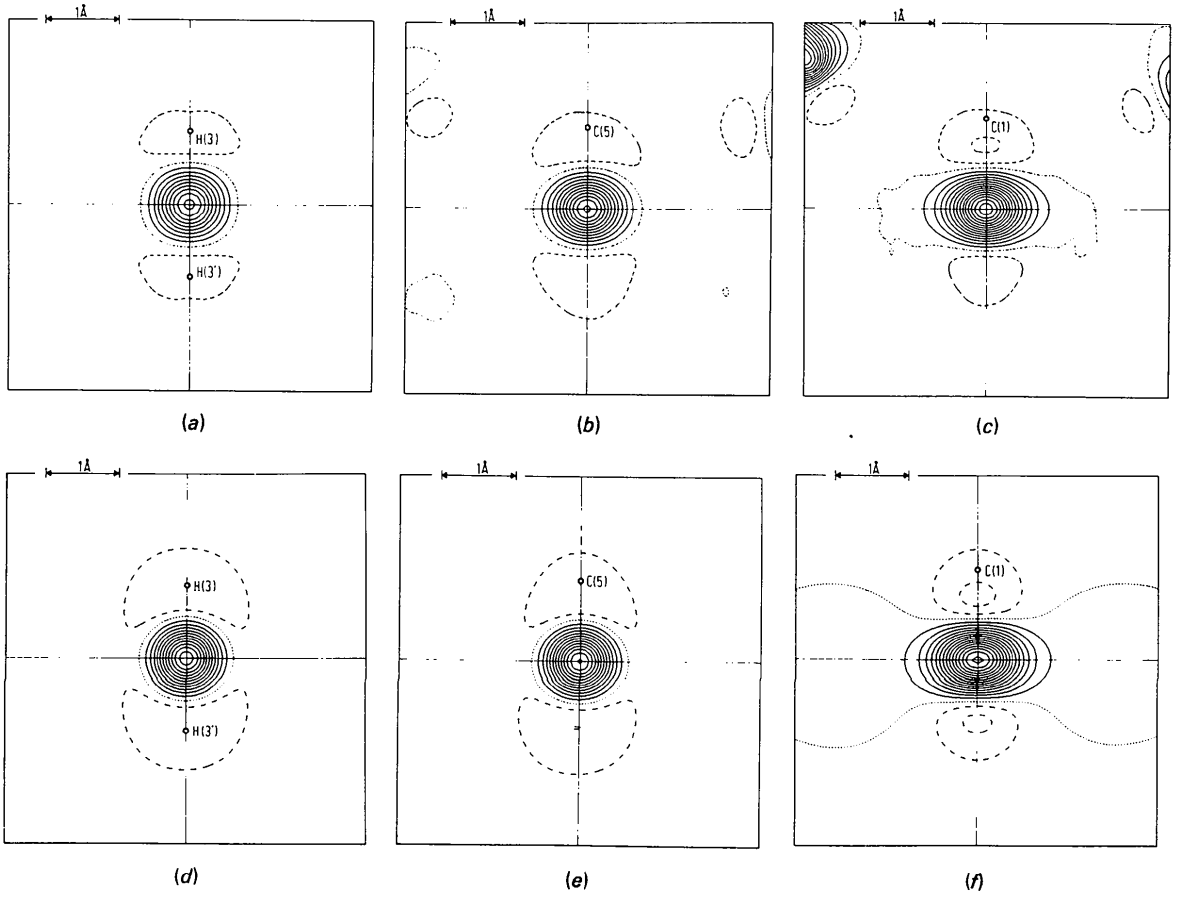

Fig. 10. $DEF^o_{exp,H}$(**r**) sections for planes perpendicular to and through the midpoint of (*a*) the BCP central bond, (*b*) the VCP central bond and (*c*) the VCP double bond, with comparable sections of $DEF^o_{th,EG}$(**r**) given in (*d*), (*e*), (*f*) respectively. The horizontal line is the direction perpendicular to the (pseudo-) mirror plane (π direction).

Foundation for Chemical Research (SON) with financial aid from the Netherlands Organization for the Advancement of Pure Research (ZWO).

References

BASCH, H., ROBIN, M. B., KUEBLER, N. A., BAKER, C. & TURNER, D. W. (1969). *J. Chem. Phys.* **51**, 52–66.

BASTIANSEN, O., FRITSCH, F. N. & HEDBERG, K. (1964). *Acta Cryst.* **17**, 538–543.

BRUCKMANN, P. & KLESSINGER, M. (1974). *Chem. Ber.* **107**, 1108–1125.

BUXTON, L. W., ALDRICH, P. D., SHEA, J. A., LEGON, A. C. & FLYGARE, W. C. (1981). *J. Chem. Phys.* **75**, 2681–2686.

CARREIRA, L. A., TOWNS, T. G. & MALLOY, T. B. (1978). *J. Am. Chem. Soc.* **100**, 385–388.

CODDING, E. G. & SCHWENDEMAN, R. H. (1974). *J. Mol. Spectrosc.* **49**, 226–231.

COULSON, C. A. (1972). *Valence*, pp. 270–271. Oxford Univ. Press.

DE MARÉ, G. R. & LAPAILLE, S. (1980). *Org. Magn. Reson.* **13**, 75–76.

DE MARÉ, G. R. & PETERSON, M. R. (1982). *J. Mol. Struct.* **89**, 213–225.

DUNCAN, J. L. (1974). *Mol. Phys.* **28**, 1177–1191.

HAGEN, K., HAGEN, G. & TRÆTTEBERG, M. (1972). *Acta Chem. Scand.* **26**, 3649–3661.

HUANG, M. B. & PAN, D. K. (1984). *J. Mol. Struct.* **108**, 49–58.

JOHNSON, C. K. (1976). *ORTEP*II. Report ORNL-5138. Oak Ridge National Laboratory, Tennessee, USA.

KEULEN, E. (1969). PhD Thesis. Univ. of Groningen, The Netherlands.

KUCHITSU, K., FUKUYAMA, T. & MORINO, Y. (1968). *J. Mol. Struct.* **1**, 463–479.

LEGON, A. C., ALDRICH, P. D. & FLYGARE, W. H. (1982). *J. Am. Chem. Soc.* **104**, 1486–1490.

MASLEN, E. N., TOIA, R. F., WHITE, A. H. & WILLIS, A. C. (1975). *J. Chem. Soc. Perkin Trans* 2, pp. 1684–1689.

MEIJERE, A. DE, LÜTTKE, W. & HEINRICH, F. (1974). *Justus Liebigs Ann. Chem.* pp. 306–327.

MEYER, A. Y. & PASTERNAK, R. (1977). *Theor. Chim. Acta*, **45**, 45–52.

MURAI (1952). *Prog. Theor. Phys.* **7**, 345.

NIJVELDT, D. & VOS, A. (1988*a*). *Acta Cryst.* B**44**, 281–289.

NIJVELDT, D. & VOS, A. (1988*b*). *Acta Cryst. B***44**, 289–296.

OVERBEEK, A. R., OLTHOF, G. J., VAN DER PUTTEN, N. & SCHENK, H. (1978). *Cryst. Struct. Commun.* **7**, 679–682.

ROOS, B. & SIEGBAHN, P. (1970*a*). *Theor. Chim. Acta*, **17**, 209–215.

ROOS, B. & SIEGBAHN, P. (1970*b*). *Theor. Chim. Acta*, **17**, 199–208.

ROOTHAAN, C. C. J. (1951). *Rev. Mod. Phys.* **23**, 69–89.

SCHOMAKER, V. & TRUEBLOOD, K. N. (1968). *Acta Cryst.* B**24**, 63–76.

SKANCKE, A. & BOGGS, J. E. (1979). *J. Mol. Struct.* **51**, 267–274.

THOLE, B. T. & VAN DUIJNEN, P. T. (1979). *BIGMOL*. Laboratory of Chemical Physics, Univ. of Groningen, The Netherlands.

TRÆTTEBERG, M. (1983). Private communication.

VELDE, G. A. VAN DER (1974). PhD Thesis. Univ. of Groningen, The Netherlands.

VON ASMUS, P. & KLESSINGER, M. (1976). *Angew. Chem.* **88**, 343–344.

VON BAEYER, A. (1885). *Ber. Dtsch. Chem. Ges.* **18**, 2269–2281.

WALSH, A. D. (1949). *Trans. Faraday Soc.* **45**, 179–190.

Acta Cryst. (1988). B**44**, 307–315

Structure and Molecular Orbital Study of Ergoline Derivatives. 1-(6-Methyl-8β-ergolinylmethyl)imidazolidine-2,4-dione (I) and 2-(10-Methoxy-1,6-dimethyl-8β-ergolinyl)ethyl 3,5-Dimethyl-1*H*-2-pyrrolecarboxylate Toluene Hemisolvate (II) and Comparison with Nicergoline (III)

BY E. FORESTI AND P. SABATINO

Dipartimento di Chimica G. Ciamician, Università di Bologna, 40126 *Bologna, Italy*

L. RIVA DI SANSEVERINO

Dipartimento di Scienze Mineralogiche, Università di Bologna, 40126 *Bologna, Italy*

R. FUSCO AND C. TOSI

Istituto G. Donegani, 28100 *Novara, Italy*

AND R. TONANI

Farmitalia Carlo Erba, 20146 *Milano, Italy*

(*Received* 18 *June* 1987; *accepted* 8 *December* 1987)

Abstract

(I): $C_{19}H_{22}N_4O_2$ (Registry No. 95688-34-9), m.p. > 573 K, $M_r = 338{\cdot}4$, orthorhombic, $P2_12_12_1$, $a = 8{\cdot}392\ (2)$, $b = 13{\cdot}004\ (2)$, $c = 15{\cdot}676\ (5)$ Å, $V = 1710{\cdot}7\ (7)$ Å^3, $Z = 4$, $D_x = 1{\cdot}31$ Mg m^{-3}, Mo $K\alpha$ radiation, $\lambda = 0{\cdot}71069$ Å, $\mu = 0{\cdot}08$ mm^{-1}, $F(000) = 720$, $T = 293$ K, final $R = 0{\cdot}051$ for 990 independent reflexions. (II): $C_{26}H_{33}N_3O_3{\cdot}\frac{1}{2}C_7H_8$ (Registry No. 54370-23-9), m.p. 427–429 K, $M_r = 481{\cdot}64$, monoclinic, $P2_1$,

0108-7681/88/030307-09$03.00